

Resonant Raman scattering in InP/In_{0.48}Ga_{0.52}P quantum dot structures embedded in a waveguide

A. A. Sirenko

*Max-Planck-Institut für Festkörperforschung, Heisenbergstraße 1, D-70569 Stuttgart, Germany
and Pennsylvania State University, 104 Davey Laboratory, University Park, Pennsylvania 16802*

M. K. Zundel, T. Ruf, K. Eberl, and M. Cardona

Max-Planck-Institut für Festkörperforschung, Heisenbergstraße 1, D-70569 Stuttgart, Germany

(Received 13 July 1998)

We report on Raman scattering in nanostructures with InP quantum dots in an In_{0.48}Ga_{0.52}P matrix embedded in an In_{0.48}Al_{0.52}P waveguide. At resonant excitation with the quantum dot excitons, broad Raman peaks corresponding to acoustic and optical vibrations were observed. Their polarization was studied for in-plane propagation of the exciting and scattered light in forward scattering geometry. In comparison with the conventional backscattering configuration, the Raman signals are drastically enhanced due to the increased scattering volume. [S0163-1829(98)01643-9]

The optical properties of quasi-zero-dimensional nanostructures are presently of great interest. Several techniques yield semiconductor quantum dots (QD's) with a well-defined and tunable size distribution. Examples are (i) QD's embedded in a glass matrix grown by diffusion-controlled phase decomposition of solid solutions,¹ (ii) QD's grown by methods of colloidal chemistry,²⁻⁴ and (iii) epitaxially grown QD's using the Stranski-Krastanov ("self-organized") growth mode.⁵⁻⁷ The first two methods, which have been mostly applied to II-VI semiconductors, produce a three-dimensional distribution of nearly spherical nanocrystals with radii from 1 to 10 nm. The last technique leads to the formation of two-dimensional arrays of pyramid-shaped QD's that typically have a base width of 10–20 nm and a height of 2–5 nm. Recently, the vibrational properties of both spherical^{1,8-10} and pyramidal¹¹⁻¹³ QD's have been extensively studied by resonant Raman scattering, which is an effective method, especially for nanocrystals distributed in a volume. For example, the confinement of optical vibrations, which can be described macroscopically as being due to a difference in the bulk dispersions and the dielectric properties of the QD material and the matrix,¹⁴⁻¹⁶ has been experimentally observed in CdSe QD's.^{1,16}

For quasi-two-dimensional arrays of nanocrystals, however, conventional backscattering experiments are limited by the small scattering volume of the QD's, and problems similar to Raman studies on thin films appear.¹⁷ Moreover, the surrounding matrix usually has Raman-active vibrations as well. Since it is probed in a much larger scattering volume, strong background signals appear which complicate or even impede the analysis of the QD response. Several experimental approaches can be used to improve the situation. For self-organized systems one can enhance the Raman signal of interest by growing stacks of quantum dot layers.^{5,18} However, this increases the scattering volume only linearly with the number of QD sheets. A significant signal enhancement can be achieved by tuning the laser excitation in resonance with excitonic QD states or by applying interference-enhanced Raman scattering¹⁹ combined with multichannel detection.¹⁷

The latter approach has been recently used in Raman studies of isolated carbon nanocrystallites.²⁰ Another possibility to obtain strong QD Raman signals is to use a waveguide geometry where the exciting and scattered light propagate along the QD sheets embedded between cladding layers. This increases the scattering volume of the low-dimensional objects enormously. In a waveguide configuration, Raman scattering by optical phonons has been recently studied in GaAs/AlAs multiple quantum wells²¹ and in LiNbO₃ thin films.²²

In this paper we report on Raman studies of self-organized InP QD's in an In_{0.48}Ga_{0.52}P matrix where the exciting and scattered photons are guided by In_{0.48}Al_{0.52}P cladding layers. The observed resonant enhancement of Raman scattering by optical and acoustic phonons as well as the corresponding polarization effects are discussed. The spectra are compared with those of bulk In_{0.5}Ga_{0.5}P.^{23,24}

Samples were grown by solid-source molecular-beam epitaxy on (001)-oriented GaAs substrates. One specimen (sample 1) contains a single layer of InP quantum dots symmetrically placed in an In_{0.48}Ga_{0.52}P matrix, lattice-matched to GaAs, with a total thickness of 0.13 μm. Another one (sample 2) consists of three layers of dots separated by 4 nm of In_{0.48}Ga_{0.52}P. The average amount of InP in a single QD layer is equivalent to a uniform coverage of 3.0 monolayers (ML). The growth process is described in detail in Refs. 7 and 18. The average QD size is approximately 3 nm in height and 16 nm in base length. The dot concentration is about 5 × 10¹⁰ cm⁻². The 0.13-μm-thick In_{0.48}Ga_{0.52}P matrix containing the QD's was surrounded by two 1-μm-thick In_{0.48}Al_{0.52}P cladding layers. These layers have a lower refractive index than the In_{0.48}Ga_{0.52}P matrix, and thus the whole structure acts as a waveguide for transmission along the plane. Note that these samples were designed to operate as semiconductor lasers under optical pumping.²⁵ Their photoluminescence (PL) spectra have been systematically studied. They exhibit a broad PL band due to QD excitons. It is centered around 1.76 eV and has a full width at half maxi-

imum (FWHM) of about 30 meV, which reflects the size distribution of the dots.¹⁸

Raman experiments were carried out with the samples at a temperature $T=10$ K. Tuneable Ti-sapphire and dye (DCM) lasers were used for excitation within the energy distribution of the QD excitons. Raman spectra were measured with a SPEX 1404 double monochromator and a DILOR XY spectrometer, equipped with a cooled GaAs photomultiplier and a charge-coupled device detector, respectively. Both the intensity and the linear polarization of the Raman signals were analyzed in the conventional backscattering configuration (laser beam and scattered light parallel to the sample growth direction z) as well as for in-plane propagation. In the following, $y' \parallel (110)$ is the direction of the exciting light for in-plane propagation and $x' \parallel (1\bar{1}0)$. The laser spot had a diameter of about $50 \mu\text{m}$; the propagation length of the light along the waveguide was about 1 mm.

Figure 1(a) shows resonant Raman spectra in the optical-phonon frequency range measured in three different scattering configurations. The excitation energy of 1.76 eV coincides with the maximum of the PL spectrum obtained at nonresonant excitation [see the solid line in Fig. 2(b)]. In the backscattering configuration $z(x',x')\bar{z}$ we observe the GaP-like longitudinal optical (LO) (383 cm^{-1}) and the InP-like LO (363 cm^{-1}) and transverse optical (TO) phonons (330 cm^{-1}) from the $\text{In}_{0.48}\text{Ga}_{0.52}\text{P}$ matrix as well as the LO phonon from the GaAs substrate (296 cm^{-1}). This spectrum does not change when the excitation energy varies over a wide range of about ± 100 meV around the QD exciton transition. It reproduces the optical-phonon spectrum of bulk $\text{In}_{0.5}\text{Ga}_{0.5}\text{P}$ epilayers.²³

For in-plane propagation of the exciting and scattered light (other configurations in Fig. 1), the spectra change. They consist of maxima at about 330 and 370 cm^{-1} , near the InP-like TO mode and in between the InP- and GaP-like LO phonons, respectively. The FWHM of these maxima is about 30 cm^{-1} . The LO maximum at 370 cm^{-1} is strongly polarized in the $y'(x',x')y'$ configuration [Fig. 1(a)] where it is about two orders of magnitude stronger than in the $y'(x',z)y'$, $y'(z,x')y'$, and $y'(z,z)y'$ geometries [Fig. 1(b)]. In the crossed polarization configuration $y'(x',z)y'$, the TO band around 330 cm^{-1} is almost as strong as the LO maximum. In the in-plane backscattering configuration $y'(x',x')\bar{y}'$ [bottom spectrum of Fig. 1(a), shown enlarged by a factor of 100] a similar broad maximum at about 370 cm^{-1} is observed. However, due to the complicated alignment (the Raman signal was optimized by maximizing the intensity of the light transmitted through the waveguide), the total intensity is much lower, a fact which limits the data analysis. Hereafter, we therefore discuss only results obtained in the forward-scattering configuration. Note that we did not find qualitative differences in the Raman spectra of samples 1 and 2, and therefore only data for sample 1 (single QD layer) will be discussed.

Resonant excitation in an in-plane geometry is required in order to observe the broad maxima at 330 and 370 cm^{-1} . Figure 2(a) shows several spectra with normalized peak intensities measured at excitation energies around the PL maximum (1.76 eV). A weak fine structure of these maxima with a modulation period of about 1.5 cm^{-1} is due to Fabry-

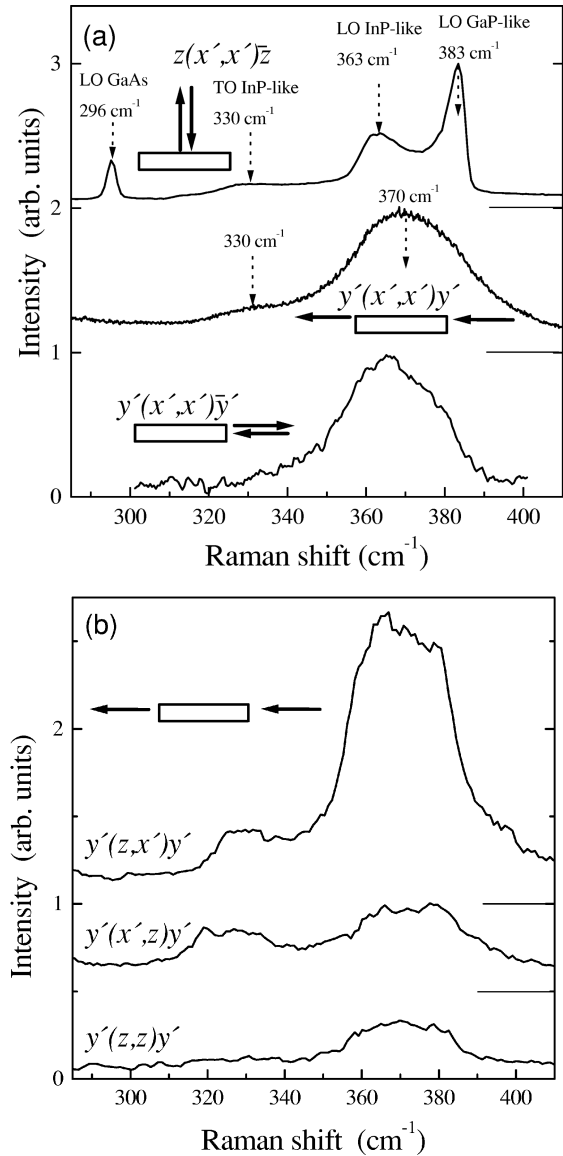


FIG. 1. (a) Resonant Raman spectra for a sample with a single layer of InP QD's (sample 1), measured with resonant excitation at 1.76 eV. In the $z(x',x')\bar{z}$ spectra a linear PL background has been subtracted for clarity. (b) Raman spectra for in-plane propagation of the exciting and scattered light. Before plotting, these spectra and the $y'(x',x')\bar{y}'$ curve in (a) were multiplied by a factor of 100 in order to facilitate the comparison with the $y'(x',x')y'$ spectrum in (a). The spectra were vertically shifted for clarity; the respective zero-signal levels are indicated by the horizontal solid lines.

Perot interferences over the 1 mm length of the sample along the y' direction.²¹ When the excitation energy departs from the resonance, the Raman lines at 363 and 383 cm^{-1} , typical for the $\text{In}_{0.48}\text{Ga}_{0.52}\text{P}$ matrix, become dominant. The intensity of the LO maximum at 370 cm^{-1} vs the excitation energy is shown by the filled squares in Fig. 2(b). It closely follows the luminescence spectrum (solid line). The dashed line in Fig. 2(b) represents the transmission spectrum for in-plane propagation of light (y' direction) with x' polarization. The threshold at 1.75 eV corresponds to the absorption edge of heavy-hole-like excitons confined in the QD's.¹⁸

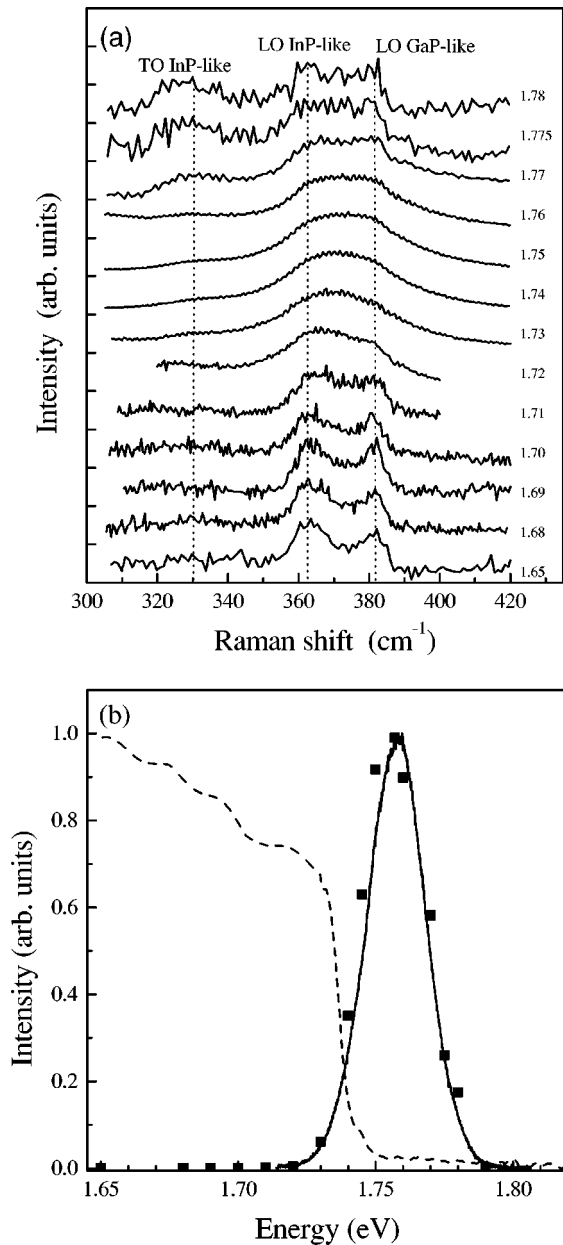


FIG. 2. (a) Raman spectra [$y'(x',x')y'$ configuration] excited around the resonance of the InP QD exciton. The respective laser energies are given in eV next to the spectra which were normalized before plotting. The vertical dashed lines guide the eye and mark the position of the optical phonons of the $\text{In}_{0.48}\text{Ga}_{0.52}\text{P}$ matrix. (b) Solid line: PL from InP quantum dots measured in the $z(x',x')z$ configuration under nonresonant excitation; dashed line: transmission spectrum in $y'(x',x')y'$ configuration; filled squares: intensity of the LO-phonon peak at 370 cm^{-1} vs excitation energy. The relative intensities of the spectra in (a) can be obtained from these data.

We also observe a weak second-order replica (2LO) of the 370 cm^{-1} LO peak at about 740 cm^{-1} . The corresponding spectrum is shown in Fig. 3. The ratio of the first- to second-order scattering intensities is about 40 for incoming resonance with the QD excitons. This strong multiphonon scattering is characteristic of resonantly excited Raman processes in low-dimensional systems.²⁶

In the acoustic-phonon frequency range, superimposed on the luminescence background, two peaks appear at 57 and

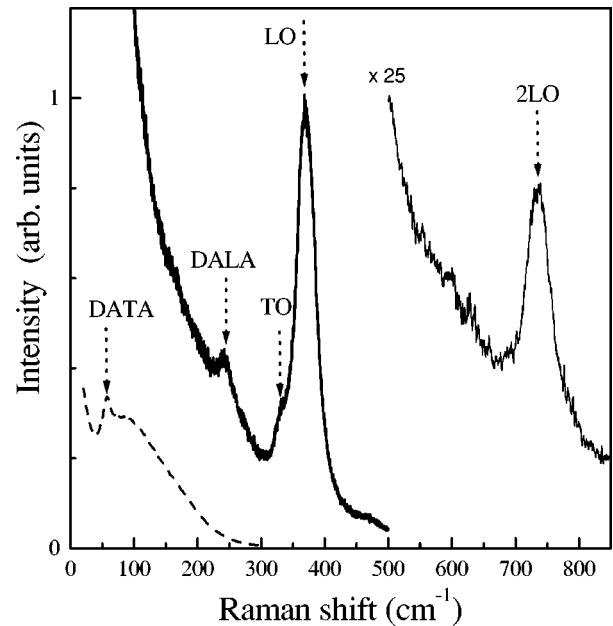


FIG. 3. Raman spectra with peaks due to acoustic and optical phonons measured in the $y'(x',x')y'$ (solid line) and $y'(z,x')y'$ (dashed line) configurations. See text for details.

240 cm^{-1} (see Fig. 3). We attribute them to the disorder-activated transverse acoustic (DATA) and longitudinal acoustic (DALA) bands, which appear in the Raman spectrum of bulk $\text{In}_{0.5}\text{Ga}_{0.5}\text{P}$ at 80 and 200 cm^{-1} , respectively.²⁴ The origin of the discrepancy in the mode frequencies is unclear at present. Note, however, that the DATA and DALA maxima depend on the $\text{In}_x\text{Ga}_{1-x}\text{P}$ composition x , and, e.g., in pure InP the corresponding values are 62 and 167.5 cm^{-1} , respectively.²⁷ The polarization of the acoustic-phonon peaks differs from that of the optical modes. The maximum at 57 cm^{-1} can be seen only in $y'(z,x')y'$ geometry, while the 240 cm^{-1} peak appears most strongly in the $y'(x',x')y'$ configuration.

For resonantly excited in-plane scattering we thus observe four Raman peaks at 57, 240, 330, and 370 cm^{-1} . The resonance profiles for the last three peaks nearly coincide with the QD PL spectrum [see Fig. 2(b)], while that of the first peak, which also has a different polarization behavior, is shifted by about 10 meV towards higher energies. This indicates that the four peaks are related to the InP QD's. The strong enhancement of the Raman signal in the $y'(x',x')y'$ geometry results from an effective coupling of the light with the heavy-hole-like QD exciton ground state, whose periodic part of the wave function has X and Y components.²⁸ The shift of the resonance curve for the peak at 57 cm^{-1} is probably due to a resonance with excited light-hole-like QD excitons, which contain significant Z contributions in their wave function. The polarization of the TA phonon signal, which is forbidden in the parallel configuration, supports this interpretation.

Quantum dots break the translational symmetry of a crystal to a certain degree. As a result, \mathbf{k} -vector conservation is relaxed in Raman processes which involve QD excitons as intermediate states.^{29–31,16} Along these lines, the large width of the peaks at 330 and 370 cm^{-1} can be partially explained by contributions from the entire TO and LO dispersion

branches of $\text{In}_x\text{Ga}_{1-x}\text{P}$ to the Raman spectrum. This is supported by measurements of disorder-activated LO and TO phonons in bulk InP where widths of about 15 cm^{-1} have been observed,²⁷ comparable to the FWHM of the 330 and 370 cm^{-1} maxima. For long-wavelength optical phonons, the InP QD's can be considered as a strong compositional disorder of the $\text{In}_x\text{Ga}_{1-x}\text{P}$ matrix, and the InP-like and GaP-like phonon frequencies can, in principle, fluctuate between the values for bulk InP and $\text{In}_{0.48}\text{Ga}_{0.52}\text{P}$.

An exact analysis of the optical-phonon spectra should take into account (i) the strain between the InP dots and the matrix, which in this system is around $3-3.5\text{ GPa}$,³² (ii) the excitation of interface modes (IF, modes involving shape effects on the electrostatic interaction), and (iii) the possible confinement of bulklike modes in InP QD's. For a single interface, IF vibrations propagate in the frequency interval between the TO and LO modes of one material (InP or $\text{In}_{0.48}\text{Ga}_{0.52}\text{P}$) if the dielectric constant of the other one has the opposite sign.³³ The peak at 370 cm^{-1} thus may have a contribution due to IF modes. Polarization selection rules allow scattering by both LO and IF modes in the same $[y'(x',x')y']$ configuration.²¹ We have not found Raman features related to confined InP-like LO or TO QD phonons which are expected around 348.5 and 306 cm^{-1} , the bulk InP

phonon frequencies, respectively.²⁷ The reason for this might be related to the strong dispersion overlap of the QD and matrix phonons.

In conclusion, for resonant excitation at QD exciton energies and for in-plane propagation of the exciting and scattered light in a waveguide configuration, we have observed Raman peaks corresponding to acoustic and optical phonons in InP QD/ $\text{In}_{0.48}\text{Ga}_{0.52}\text{P}$ matrix structures. In comparison with the conventional backscattering geometry, which only shows the peaks expected from the two-mode behavior of the $\text{In}_{0.48}\text{Ga}_{0.52}\text{P}$ matrix, strong Raman signals from processes involving both the matrix and the QD system have been obtained. These features result from the combination of relaxed crystal-momentum conservation in the InP QD's, the resonant excitation conditions, and the large number of QD's probed.

The authors are grateful to J. Fox for discussions. Thanks are due to P. Hiessl, H. Hirt, and M. Siemers for their help with the experiment and to L. Lastras for a critical reading of the manuscript. A. A. Sirenko would like to thank the Alexander von Humboldt Foundation, the NSF (Grant No. DMR-9623315), and the DOE (Grant No. DE-FG02-84ER45095) for financial support.

-
- ¹A. Ekimov, *J. Lumin.* **70**, 1 (1996).
²C. B. Murray *et al.*, *Science* **270**, 1335 (1995).
³A. A. Guzelian *et al.*, *Appl. Phys. Lett.* **69**, 1432 (1996).
⁴D. Bertram *et al.*, *Phys. Rev. B* **57**, 4265 (1998).
⁵M. Grundmann *et al.*, *Phys. Status Solidi B* **188**, 249 (1995).
⁶N. N. Ledentsov *et al.*, *Solid-State Electron.* **40**, 785 (1996).
⁷A. Kurtenbach *et al.*, *Appl. Phys. Lett.* **66**, 361 (1995).
⁸A. P. Alivisatos *et al.*, *J. Chem. Phys.* **90**, 3463 (1989).
⁹M. C. Klein *et al.*, *Phys. Rev. B* **42**, 11 123 (1990).
¹⁰A. Tanaka *et al.*, *Phys. Rev. B* **45**, 6587 (1992).
¹¹R. Heitz *et al.*, *Appl. Phys. Lett.* **68**, 361 (1995).
¹²B. R. Bennett *et al.*, *Appl. Phys. Lett.* **68**, 958 (1996).
¹³J. Groenen *et al.*, *Appl. Phys. Lett.* **69**, 943 (1996).
¹⁴E. Roca *et al.*, *Phys. Rev. B* **49**, 13 704 (1994).
¹⁵E. Menéndez *et al.*, *Phys. Status Solidi B* **199**, 81 (1997).
¹⁶C. Trallero-Giner *et al.*, *Phys. Rev. B* **57**, 4664 (1998).
¹⁷J. C. Tsang, in *Light Scattering in Solids V*, edited by M. Cardona and G. Güntherodt, *Topics in Applied Physics Vol. V* (Springer-Verlag, Berlin, 1989), Chap. 6, p. 233.
¹⁸M. K. Zundel *et al.*, *Appl. Phys. Lett.* **71**, 2972 (1997).
¹⁹G. A. N. Connel *et al.*, *Appl. Phys. Lett.* **36**, 31 (1980).
²⁰V. I. Merkulov *et al.*, in *Advances in Microcrystalline and Nanocrystalline Semiconductors*, edited by R. W. Collins *et al.*, *Materials Research Society Symposia Proceedings No. 452* (MRS, Pittsburgh, 1996), p. 225.
²¹A. Fainstein *et al.*, *Phys. Rev. B* **51**, 14 448 (1995).
²²I. Savatinova *et al.*, *J. Phys. D* **25**, 106 (1992).
²³A. Hassine *et al.*, *Mater. Sci. Eng., B* **28**, 151 (1994).
²⁴A. Hassine *et al.*, *Phys. Rev. B* **54**, 2728 (1996).
²⁵A. Moritz *et al.*, *Appl. Phys. Lett.* **69**, 212 (1996).
²⁶D. J. Mowbray *et al.*, *Phys. Rev. B* **43**, 11 815 (1991).
²⁷E. Bedel *et al.*, *J. Phys. C* **19**, 1471 (1986).
²⁸M. Cardona *et al.*, *Phys. Rev. B* **38**, 1806 (1988).
²⁹P. S. Kop'ev *et al.*, *Pis'ma Zh. Éksp. Teor. Fiz.* **51**, 624 (1990) [*JETP Lett.* **51**, 708 (1990)].
³⁰V. F. Sapega *et al.*, *Phys. Rev. B* **46**, 16 005 (1992).
³¹A. A. Sirenko *et al.*, *Phys. Rev. B* **58**, 2077 (1998).
³²C. Ulrich *et al.*, *Phys. Rev. B* **52**, 12 212 (1995).
³³A. K. Sood *et al.*, *Phys. Rev. Lett.* **54**, 2115 (1985).